

Analysis of Atlantic extratropical storm tracks characteristics in 41 years of ERA5 and CFSR/CFSv2 databases

Article

Accepted Version

Creative Commons: Attribution-Noncommercial-No Derivative Works 4.0

Gramscianinov, C. B., Campos, R. M., de Camargo, R., Hodges, K., Guedes Soares, C. and da Silva Dias, P. L. (2020) Analysis of Atlantic extratropical storm tracks characteristics in 41 years of ERA5 and CFSR/CFSv2 databases. *Ocean Engineering*, 216. 108111. ISSN 0029-8018 doi: <https://doi.org/10.1016/j.oceaneng.2020.108111> Available at <https://centaur.reading.ac.uk/92935/>

It is advisable to refer to the publisher's version if you intend to cite from the work. See [Guidance on citing](#).

To link to this article DOI: <http://dx.doi.org/10.1016/j.oceaneng.2020.108111>

Publisher: Elsevier

All outputs in CentAUR are protected by Intellectual Property Rights law, including copyright law. Copyright and IPR is retained by the creators or other copyright holders. Terms and conditions for use of this material are defined in the [End User Agreement](#).

www.reading.ac.uk/centaur

CentAUR

Central Archive at the University of Reading

Reading's research outputs online

Analysis of Atlantic extratropical storm tracks characteristics in 41 years of ERA5 and CFSR/CFSv2

C.B. Gramscianinov^{12*}, R.M. Campos¹, R. de Camargo², K.I. Hodges³, C. Guedes Soares¹, P.L. da Silva Dias²

¹*Centre for Marine Technology and Ocean Engineering (CENTEC), Instituto Superior Técnico, Universidade de Lisboa. Rovisco Pais, 1049-001 Lisboa, Portugal.*

²*Departamento de Ciências Atmosféricas, Instituto de Astronomia, Geofísica e Ciências Atmosféricas, Universidade de São Paulo, Rua do Matão 1226, Cidade Universitária, São Paulo, SP, Brazil.*

³*Department of Meteorology, University of Reading, Reading, United Kingdom.*

*Corresponding Author, e-mail address: cbgramscianinov@gmail.com

ABSTRACT: This work aims to analyze and compare ERA5 and CFSR/CFSv2 from 1979 to 2019 with 1-hourly outputs, regarding their ability to reproduce storm tracks and the main characteristics of **cyclones at middle and high latitudes** in the North Atlantic (NA) and South Atlantic (SA) Oceans. The cyclone tracking was based on relative vorticity at 850 hPa and the intensity is measured using the maximum 10-meter wind speed. The climatology produced for both datasets shows the main characteristics of the NA and SA storm tracks, such as seasonal variability and genesis regions. The use of 1-hourly fields improves tracking in areas with complex terrains, such as the lee of Andes (SA) and Greenland (NA). The differences in cyclone numbers and characteristics between datasets are small. 92.7% and 93.1% of ERA5 cyclones have an identical correspondent storm in CFSR/CFSv2, in the NA and SA respectively. Genesis and lifetime statistics show that CFSR/CFSv2 may present inconsistency between forecast and analysis sequential time-steps. Large differences remain in the intensity distributions, in which the CFSR/CFSv2 presents stronger cyclones than ERA5. Divergences between the datasets decrease when the comparison is made using only CFSv2, particularly in the South Atlantic.

Keywords: Extratropical cyclones; storm tracks; cyclogenesis; South Atlantic Ocean; North Atlantic Ocean; reanalysis.

1. Introduction

Cyclones are key features of the day-to-day weather variability at middle and high latitudes. Storminess is an important risk for offshore structures and ship routing, particularly due to their associated extreme winds and waves (Ponce de León and Guedes Soares, 2012; Vettor and

Guedes Soares, 2016; 2017). Safe and profitable engineering operations depend on weather forecasts and metocean statistics, the last being usually produced from reanalysis data produced by operational centers around the world (Campos et al., 2018; 2019). Transient system variability in the extratropics are the contributor to not only errors in wind-wave forecasts but also for problems associated with the representation of topographic and sea surface temperature gradient effects in ocean models (Chelton et al., 2004). Cyclone tracks are usually obtained using 6-hourly data sources, which are necessary to produce reliable cyclone tracks but are insufficient for some ocean engineering problems, such as wave hindcast and forecast models. In this paper **cyclone tracks** in the Atlantic Ocean from two modern reanalysis datasets are compared, the fifth generation of reanalysis from the European Centre for Medium-Range Weather Forecast (ECMWF; Hersbach and Dee, 2016) (ERA5), and the Climate Forecast System Reanalysis (CFSR; Saha et al., 2011), and Climate Forecast System version 2 (CFSv2; Saha et al., 2014) from the National Center for Environmental Prediction (NCEP). Besides the analysis of these two datasets and the discussion, an important contribution of this work is to produce **a cyclone** database that can be used to support ocean engineering and coastal hazard estimations, together with an evaluation of the main differences between the two datasets.

Automated methods for cyclone identification and tracking have been developed in the past decades, due to the increase of available data produced by Global Circulation Models (GCMs) and reanalyses, led by the improvement of computational resources. These objective methods are based on a Lagrangian approach that generally uses low-level vorticity or surface pressure criteria to identify and track cyclones (e.g., Murray and Simmonds, 1991; Sinclair, 1994; Hodges, 1994; 1995). Since then, a wide set of cyclone climatologies have been produced for the Northern Hemisphere (e.g., Hoskins and Hodges, 2002), Southern Hemisphere (e.g., Jones and

45 Simmonds 1993; Sinclair 1994; Simmonds and Keay, 2000; Hoskins and Hodges, 2005), North
46 Atlantic (e.g., Pinto et al., 2005; Trigo, 2006; Dacre and Gray, 2009, Grise et al., 2013), and
47 South Atlantic Oceans (e.g., Mendes et al., 2010, Reboita et al., 2010, Gramscianinov et al.,
48 2019). The basic product of the tracking method is the collection of cyclone trajectories within a
49 defined region and period. The spatial statistic distribution of this collection of trajectories
50 defines the storm track position – the preferred location of **cyclone** propagation.

51 Following the development of GCMs, the use of analyses and reanalyses was a valuable
52 improvement to the atmosphere and ocean dynamics studies (Parker, 2016). Reanalysis products
53 are based on a model allied to data assimilation, and thus, can provide a complete spatial
54 coverage at a regular resolution. Despite the verification and validation performed by
55 development centers (e.g., Kalnay et al., 1996; Saha et al., 2011; 2014), it is important to
56 evaluate the performance of these datasets for particular applications, such as extratropical and
57 tropical cyclones, and precipitation. Several studies have carried out intercomparisons of storm
58 tracks obtained from different datasets for the whole globe (e.g., Hodges et al., 2003; 2011),
59 Northern Hemisphere (e.g., Raible et al., 2008), North Atlantic sector (e.g., Trigo, 2006) and
60 South Atlantic sector (Reboita et al., 2018; Crespo et al., 2020a). Hodges et al. (2011) compared
61 the storm track distribution and intensity in four reanalysis: the Modern Era Retrospective-
62 Reanalysis for Research and Applications (MERRA; Rienecker et al., 2011), the 25-yr Japan
63 Reanalysis (JRA25; Onogi et al., 2007), the ECMWF Interim Reanalysis (ERA-Interim;
64 Simmons et al. 2007), and the CFSR. They found larger discrepancies between the older and
65 newer products and attributed their findings to the improvement of data assimilation techniques
66 and increase of resolution. According to them, modern reanalysis inter compares better than the
67 older ones for cyclone densities. However, differences remain large between CFSR and ERA-

Interim for cyclones intensities, and also for densities in some regions of the Southern Hemisphere. Stopa and Cheung (2014) evaluated 30 years of wind and wave data from the CFSR and ERA-Interim using altimeter and buoy observations. While ERA-Interim presented lower error metrics, CFSR showed a better performance in the upper percentiles associated with extreme events. The large differences between datasets are generally associated with the failure in the representation of extreme events (e.g., Stopa and Cheung, 2014; Campos et al., 2018). Winds are often underestimated at some locations, mainly in the Southern Hemisphere, due to the lack of observational data (e.g., Stopa and Cheung, 2014). This problem contributes to the misrepresentation of cyclones, particularly the most intense ones, which leads to issues in wind-wave climate hindcast and forecast (e.g., Kumar et al., 2003; Campos and Guedes Soares, 2016; 2017; Bakhtyar et al., 2018; Mattioli et al., 2019; Campos et al., 2019), and storm surge estimations (e.g., Colle et al., 2010; Booth et al., 2016; Sebastian et al., 2019).

Therefore, it is important to evaluate cyclone and storm track characteristics of datasets available at high temporal resolution, since 1-hourly fields are frequently used to support the production of wave hindcasts and forecasts, and energy sector assessments. The main goal of this study is to present and evaluate the Atlantic cyclone climatology for middle and high latitudes that can be used by research and industry applications, since there is a lack of this type of product available (e.g., Dacre et al., 2012), particularly for the South Atlantic Ocean. Therefore, two main questions for this study are: (1) How does the 1-hourly ERA5 and CFSR/CFSv2 cyclone tracks for the Atlantic storm track compare with previously published studies?; (2) What are the main differences between the two datasets regarding the basic cyclone and storm track characteristics? The analysis is focused on the mean characteristics, spatial distribution and intensity of the cyclones, which are important features that control the wind and wave climates.

2. Data and Methods

2.1. Datasets

ERA5 is the latest reanalysis produced by ECMWF, available from the Copernicus Climate Change Service (CS3). This reanalysis has been produced using 4D-Var data assimilation in ECMWF's Integrated Forecast System (IFS), version CY41R2. The atmospheric variables used in this work are on a 31 km (0.28125°) horizontal grid with 1-hourly outputs from 1979 to 2020. ERA5 replaces the ERA-Interim, and benefits from its antecessor's development in model physics, core dynamics and data assimilation. One of the most important innovations of ERA5 is output of hourly analyses that can widely support risk and operational management in diverse sectors, such as renewable energy (e.g., Olauson, 2018). Moreover, Belmonte Rivas and Stoffelen (2019) found that ERA5 surface winds present a 20% improvement relative to ERA-Interim, using ASCAT observations as verification. An overview of the main characteristics of ERA5 and a comparison with ERA-Interim can be found in Hersbach et al. (2018).

The CFSR is the latest version of the NCEP climate reanalysis and covers the period from 1979-March/2011. The reanalysis was produced using a coupled atmosphere–ocean model: the NCEP Global Forecast System (GFS) for the atmosphere and the Geophysical Fluid Dynamics Laboratory Modular Ocean Model version 4 (MOM4) for the ocean (Saha et al., 2010). The CFSv2, the operational descendant of the CFSR, was released in March 2011, and it has been running operationally since then. The CFSR and CFSv2 have a horizontal native resolution of T382 (~ 38 km) interpolated to a $0.5^\circ \times 0.5^\circ$ grid. Both the reanalysis and analysis are produced originally in 6-hourly intervals, but a 1-hourly time series are also available from some variables and consist of the analysis followed by the sequence of hourly forecasts until the next analysis

cycle. The hourly sequence provided might have abrupt changes in atmospheric fields every time when a forecast time-step changes to analysis time-step, since the last is corrected by data assimilation. Despite this eventual inconsistency along the period, it is important to evaluate the hourly data since these products are used for ocean engineering applications. Moreover, it is the only way to compare CFSR/CFSv2 with ERA5 1-hourly data. Differences between products are expected and need to be discussed to support future choices and/or changes.

2.2. Cyclone identification and tracking

The cyclones are identified and tracked in both reanalyses using the TRACK program (Hodges, 1994; 1995; 1999) following the pre-processing steps described in Hoskins and Hodges (2002; 2005). The cyclonic features were identified using the relative vorticity, which is computed using the zonal and meridional wind components at 850 hPa in spherical coordinates to avoid latitudinal bias (Sinclair, 1997). Sinclair (1994) highlighted the benefit of using vorticity instead of mean sea level pressure (MSLP) for the detection of cyclones in mid-latitudes, where the surface pressure gradient can be strong so that cyclones appear without a closed isobar. For this reason, the use of vorticity allows the early identification of cyclones that would only be detected by MSLP when intensification occurs or they move to higher latitudes. The vorticity field contains many small scale structures, particularly at the high resolution, which can cause problems during the identification process and tracking on the synoptic scale. To prevent this issue and focus on synoptic scales, the vorticity was spectrally filtered by converting to the spectral representation and truncating to T42, tapering the spectral coefficients to smooth the data. Large-scale atmospheric features were also removed by setting zonal wavenumbers ≤ 5 to zero. Hoskins and Hodges (2002) present more details about the filtering.

The cyclonic features are identified by determining the local maxima. In the Southern Hemisphere, where negative vorticity indicates cyclonic circulation, the vorticity fields are first scaled by -1. First, the central position of the cyclonic feature is determined by the grid point maxima that exceed a threshold of $1 \times 10^{-5} \text{ s}^{-1}$ (1 cyclonic vorticity unit (CVU)) on a polar stereographic projection. This identification threshold is suitable to capture even weak cyclonic centers in the filtered vorticity field (T42), since it is smoother than the original vorticity one (e.g., Hoskins and Hodges, 2002; 2005). The feature central locations are refined by computing the off-grid maxima using B-spline interpolation and steepest descent maximization and then converted back to spherical coordinates. The tracking is initialized using a nearest neighbors search method. The initial set of tracks is refined by minimizing a cost function for track smoothness, subject to adaptive constraints (Hodges, 1999), that operates both forwards and backward in time. The high time resolution reduces ambiguity during tracking. The displacement constraint applied was 2.0° , except in the tropics (20°N - 20°S) where it was set as 0.5° . Due to the large amount of data, the tracking was performed using monthly files. Thus, post-processing was applied to connect tracks between the months, using the same displacements rules described above.

Finally, identified systems that are not cyclones were excluded. In this step, cyclonic features, such as thermal lows, mesoscale storms, and some convergence areas were removed by considering only systems that last at least 24 hours and that travel further than 1000 km, such as used by Gramscianinov et al. (2019) for the South Atlantic Ocean. The thresholds are more relaxed than the ones commonly used in North Atlantic storm track studies (e.g., Hoskins and Hodges, 2002; 2005; Hodges et al., 2011; Dacre and Gray, 2009), but it maintains consistency throughout the entire Atlantic. The use of a higher minimum lifetime threshold (e.g., 36h or 48h)

would exclude some systems with regional importance (e.g., Gramscianinov et al., 2019; 2020). Gramscianinov et al. (2020) considered cyclones with a minimum of 12h lifetime and 500km displacement, to include short-lived systems that might be important for extreme waves along the Southern Brazilian coast. However, the use of such a low displacement threshold results in including continental lows and non-developed cyclonic systems in the climatology. Figure 1 shows the genesis and track densities of cyclonic systems that live at least 24 hours with the total displacement between 500 and 1000 km. In the North Atlantic, 23% (ERA5) and 26% (CFSR/CFSv2) of the cyclonic systems were excluded with the 1000 km ($\sim 10^\circ$) displacement threshold, while in the South Atlantic they represented a smaller portion of 15% (ERA5) and 21% (CFSR/CFSv2). Although these values can be considered important, the track density reveals that systems with small mobility (semi-stationary) are mainly continental and thermal lows generated in complex terrain, and troughs that are generated in frontal zones, without enough forcing for full-development. The genesis densities are smaller when compared to active cyclone genesis regions reported in the literature (e.g., Hoskins and Hodges, 2002; 2005), and the track density is restricted to the generation point revealing the small influence of the systems, which mostly do not reach the ocean.

Since the main interest of this work is on cyclones at middle and high latitude, we considered for further analysis storms which pass within the extratropical latitudes of the South Atlantic (85°S - 25°S , 75°W - 20°E) and North Atlantic (85°N - 25°N , 65°W - 0°E). The selected domains include areas where occurs subtropical cyclones generated both by genuine subtropical genesis and by transition process between tropical and extratropical cyclones (e.g., Guishard et al., 2009; Evans and Braun, 2012; Gozzo et al., 2014). In this way, subtropical cyclones may be included in

the set of tracks, since no distinction between subtropical and extratropical cyclones was made in the present work.

2.3. Cyclone diagnostics

The statistical analysis consists of information for the tracks, including mean lifetime of cyclones, cyclone speed, and displacement. Standard seasons are used for the entire period (1979-2019): December-February (DJF), March-May (MAM), June-August (JJA), and September-November (SON). Spatial statistics are computed for each reanalysis using the spherical kernel estimator approach, described by Hodges (1996). The differences between track and genesis densities of the two datasets were tested using Monte Carlo significance test (Hodges, 2008) with 1000 samples of the set of tracks for each dataset.

Maximum 10-m wind speed is used for the comparison of cyclone intensities. The 10-m wind speed is added to each track by a general search for the maximum value within a 6° radius of cyclone center (Bengtsson et al., 2009). This additional information was used to construct maximum intensity distributions for both ERA5 and CFSR/CFSv2. Moreover, identification of matched tracks between the datasets was made to perform a more direct comparison of the cyclone intensities. A storm was considered to be the same in ERA5 and CFSR/CFSv2 when the mean separation distance between cores was less than 2° (geodesic) and they overlap in time by at 50% of their points. The criteria used here is stricter than the one applied in Hodges et al. (2011), where the minimum mean separation distance was 4° . The choice of a smaller distance agrees with the focus of this work, linked to ocean engineering applications, in which smaller differences in the system position may lead to large biases in the wind and wave fields.

3. Results

3.1. Genesis and track densities

Before the direct comparison between storms tracks in each dataset, the climatology of the cyclones is presented, using ERA5 as a reference, to provide an overview of the storm track pattern and genesis variability in the North and South Atlantic Oceans.

3.1.1. North Atlantic

The track and genesis densities in the North Atlantic domain for the entire period, boreal winter (DJF) and summer (JJA) are shown for the ERA5 and CFSR/CFSv2 in Figure 2 and Figure 3. The North Atlantic storm track is represented by the region of maximum track density [> 10 cyclones $(10^{-6}, \text{km}^2)^{-1} (\text{month})^{-1}$] extending northeastward, from the East of North American coast to Greenland and North Europe. A northern path of the storm track strengthens in DJF, along the eastern side of Greenland, due to the increase in genesis activity at this location. The genesis density shows four regions favorable to cyclogenesis [> 2 cyclones $(10^{-6}, \text{km}^2)^{-1} (\text{month})^{-1}$]: lee of the southern Rockies (35°N , 102.5°W), West Atlantic (40°N , 75°W), East Atlantic (centered at 50°N , 25°W), and in the eastern coast of Greenland.

All genesis regions within the North Atlantic domain are more active during the boreal winter (DJF). However, the genesis region along the eastern North American coast is active all year, being a location with high baroclinicity due to the sea surface temperature gradients provided by the warm Gulf Stream. The surface temperature contrast does not give only conditions to genesis but also to the intensification of pre-existing cyclones and perturbations that come from continent - which may be generated on the lee side of Rockies. Grise et al. (2013) constructed a genesis density distribution using not the first track point of each cyclone but the location where

storms exceeded the growth rate of 2 CVU per day, and they found a major genesis density along the east coast of North America and less at the Rockies. The genesis region at the lee of the northern Rockies and its consequent storm track density along the continent (e.g., Hoskins and Hodges, 2002) does not appear in Figure 3 because these cyclones dissipate in the northeast portion of the North American continent, outside the North Atlantic domain (Dacre and Gray, 2009). The genesis densities along the east Greenland coast are higher in Figure 3 than in some previous studies selecting cyclones that last more than 48 h (e.g., Hoskins and Hodges, 2002; Dacre and Gray, 2009; Grise et al., 2013). Trigo (2006) used the 24h threshold and also obtained a more pronounced genesis density in Greenland.

3.1.2. *South Atlantic*

Figure 4 and Figure 5 show the cyclone track and genesis densities in the South Atlantic for the ERA5 and CFSR/CFSv2, computed for the whole period, as well as divided into austral summer (DJF), and winter (JJA). The main South Atlantic storm track is defined by the high concentration of systems [> 10 cyclones $(10^{-6}, \text{km}^2)^{-1} (\text{month})^{-1}$] extending from west to east of the domain, between 40°S and 55°S . Furthermore, there is a secondary storm track [> 6 cyclones $(10^{-6}, \text{km}^2)^{-1} (\text{month})^{-1}$] that merges with the primary storm track, being considered a subtropical branch. During the austral summer (DJF), the subtropical storm track spreads northward, originating between 30°S and 35°S , while during the winter this branch is concentrated in 35°S . The winter season variability in the South Atlantic storm track is linked to changes in active genesis regions in South America, as is possible to see in the genesis density spatial distribution (Figure 5).

The genesis density for all period shows three main regions of active genesis [> 2 cyclones (10^{-6} , km^2) $^{-1}$ (month) $^{-1}$]: in Uruguay (35°S, 60°W), Argentinean coast (45°S, 65°W), and Antarctic Peninsula (65°S, 60°W). Secondary genesis regions exist in the Southeast Brazilian coast (27°S, 45°W), and southeast portion of South Atlantic (centered at 45°S, 10°W). The former is only pronounced during the austral summer, while the last **has more genesis during** the winter (e.g., Gramscianinov et al., 2019). In South America, the genesis regions at Uruguay are more active during JJA, while the Argentina's genesis region is more active in DJF. However, the genesis region in Argentina presents a high density of genesis during all year [> 5 cyclones (10^{-6} , km^2) $^{-1}$ (month) $^{-1}$]. The genesis region in Southeast Brazilian coast and Southeast South Atlantic are more active in CFSR/CFSv2 climatology [> 2 cyclones (10^{-6} , km^2) $^{-1}$ (month) $^{-1}$] than in ERA5.

The spatial distribution and seasonal variation presented in Figure 4 and Figure 5 are in agreement with previous studies (e.g., Hoskins and Hodges, 2005; Reboita et al., 2010; Gramscianinov et al., 2019). A more direct comparison can be made with results from Gramscianinov et al. (2019) since the system duration and displacement threshold applied are the same (24 h and 1000 km). They found a slightly more active genesis region in the Southeast Brazilian coast in DJF. Also, the Uruguay genesis region is much more active in the present work, with a genesis density almost 20% larger.

3.2.Differences between ERA5 and CFSR/CFSv2 cyclones

Table 1 shows the cyclone annual and seasonal mean frequencies computed for the entire period (1979 to 2011). Such values were also computed for the split period linked to CFSR (1979-March/2011) and CFSv2 (April/2011-2019) separately, to analyze the differences between

datasets. In general, ERA5 produces more cyclones than CFSR/CFSv2, which is expected due to the higher resolution of the former. The differences between the two datasets are smaller in the North Atlantic than in the South Atlantic in all cases. In the North Atlantic, the differences in cyclone numbers are between 0.4% and 4.4%, being the lowest and largest differences detected in MAM and JJA respectively. The period of JJA is the only season that CFSR/CFSv2 presents more cyclones than ERA5. The differences between datasets for the South Atlantic vary from 6.3% to 2.3%. The largest difference occurs in JJA, the most active cyclonic season. By choosing ERA5 as the reference, the CFSv2 improves the cyclone representation in the South Atlantic when compared to its antecessor, since there is a reduction of differences between CFSv2 and ERA5 when compared to CFSR and ERA5. It is not possible to conclude the same for the North Atlantic, which presents a small increase or decrease of differences depending on the season.

The spatial distribution and intensity differences between ERA5 and CFSR/CFSv2 are presented in the following subsections. The results focus on the storm track active season in each ocean basin: boreal winter (DJF) for the North Atlantic, and austral winter (JJA) for the South Atlantic.

3.2.1. Spatial distribution

The winter genesis and track density differences between the two datasets are presented in Figure 6 for the North Atlantic (DJF) and South Atlantic (JJA). The difference is computed as CFSR/CFSv2 minus ERA5, so positive (negative) values indicate that the CFSR/CFSv2 has more (less) genesis or tracks in a location. Areas with significant differences (p -value < 0.01) are marked with a black dot. First, for the North Atlantic, the track density difference shows that ERA5 have more storm tracks than CFSR/CFSv2. The track differences do not show any dipole

patterns that would indicate shifts between storm tracks but, instead, the negative values are distributed all over the main North Atlantic storm track paths from the eastern portion of the eastern USA to Iceland and the UK. However, there are some local differences in genesis density comparisons. The CFSR/CFSv2 presents a more concentrated genesis along the eastern coast of North American, between 40°N and 55°N, and offshore areas. This genesis difference along the coast generates an eastward shift of the east of North Atlantic genesis region between the two datasets. The CFSR/CFSv2 also presents an active genesis region closer to the UK (15°W) than ERA5 (25°W). Differences are larger in the South Atlantic, both in genesis and track densities. The track density differences show that ERA5 presents a higher track density in most of the domain, particularly where the South Atlantic storm track is typically found, between 40°S and 55°S, following the spiral pattern typical of the winter. Moreover, in the southwest of the domain, in the Drake Passage (55°S and 66°S), there is a pronounced difference associated with cyclones that come from the South Pacific Ocean. The genesis density difference shows that the cyclogenesis regions over Uruguay and Argentina are more active in ERA5, while CFSR/CFSv2 favors genesis in the oceanic portion off of South America Eastern coast and Southeast of South Atlantic. The genesis region in the Antarctic Peninsula is more active in ERA5, which are connected to more cyclonic perturbations coming from the South Pacific.

3.2.2. *Cyclone intensity and additional characteristics*

Some important cyclones characteristics are shown in Table 2 for ERA5, CFSR/CFSv2, CFSv2 and CFSR, for both oceanic basins. First, the mean initial vorticity is calculated by the filtered vorticity (T42) at the time of the genesis in each track. The CFSR/CFSv2 presents larger initial vorticity than ERA5, in all periods considered. The difference is larger for the South

Atlantic, where CFSR/CFSv2 cyclones are 10.4% more intense at the time of the genesis than cyclones in ERA5. For the North Atlantic cyclones, CFSR/CFSv2 present storms 6.4% more intense than ERA5. The cyclone propagation speed is similar between datasets, which is expected once it is mainly dictated by the large scale flow. As is possible to see, regarding cyclones' mean characteristics, the differences between ERA5 and CFSR/CFSv2 are small, and not significant due to the large variance. Analyzing CFSR and CFSv2 separately, the differences compared to ERA5 decrease in version 2. Despite the large standard deviation, the mean values indicate that ERA5 cyclones seem to live longer and move further than CFSR/CFSv2 ones. To investigate further the duration and displacement differences between the two datasets the histograms of those cyclones characteristics are presented in Figure 7. In fact, the lifetime and displacement distributions show that CFSR/CFSv2 presents a larger portion of small-distance and short-life cyclones when compared to ERA5.

The intensity distributions are shown in Figure 8 for both the North Atlantic (DJF) and South Atlantic (JJA) in two periods: from 1979 to 2019, and April/2011 to 2019, the last referring to CFSv2 solely. Figure 8 also shows the intensity distribution of the matched tracks between datasets. The percentage of matched tracks between ERA5 and CFSR/CFSv2 can be found in Table 3. The maximum 10-m wind speed distribution for all cyclones shows that the CFSR/CFSv2 presents more intense cyclones than ERA5, as its distribution is shifted to the right. The mean maximum surface winds and percentiles of the distributions are displayed in Table 4. CFSR/CFSv2 presents a higher mean and percentiles, and the differences between the datasets are larger for the South Atlantic than North Atlantic. Additionally, the CFSv2 has a broader distribution when compared to ERA5, although this is more evident in the North Atlantic. The same behavior was observed by Hodges et al. (2011) when they compared CFSR

and ERA-Interim. The tendency of CFSR/CFSv2 to simulate more intense storms is reported by previous studies (Hodges et al., 2011; Stopa and Cheung, 2014; Gramscianinov et al., 2020b). The matching storms distribution reveals more about the dissimilarities between the datasets since it compares the same storm simulated in each one. The intensity distribution of the matched tracks is very similar to the distribution obtained with all tracks, due to the high correspondence percentage between datasets (Table 3). Even for the matching cyclones distributions, CFSR/CFSv2 cyclones are more intense than ERA5 ones, reinforcing its tendency to simulate stronger storms. Analysing CFSR alone (not shown) does not change this behavior, but the intensity distributions computed for CFSv2 and ERA5 between April/2011 and 2019, present a slight increase in cyclones intensity in relation to the mean and past distribution. The distribution computed for the end of the period is shifted to the right, and has a more pronounced tail to the right side of maximum wind speed axis.

4. Discussion

The cyclone climatologies covering 41-years produced from ERA5 and CFSR/CFSv2 are in good agreement with past studies for the North Atlantic (e.g., Hoskins and Hodges, 2002; Trigo, 2006; Dacre and Gray, 2009) and South Atlantic Oceans (e.g., Hoskins and Hodges, 2005; Gramscianinov et al., 2019). Differences in genesis and track densities between the present and past studies are expected, particularly due to the use of distinct cyclone tracking methods, domains, and thresholds that define whether a cyclonic feature is a cyclone or not (Pinto et al., 2005). The climatologies presented in this work show a higher cyclone density than Hoskins and Hodges (2002, 2005), Dacre and Gray (2009), and Grise et al. (2013), since these authors remove from their climatology cyclones that live less than 48h, which represent a large portion of the

systems in this study (Figure 7). However, when compared to Trigo (2006) and Gramscianinov et al (2019), which also used the 24 hours as cyclone lifetime threshold, the densities presented in this work are comparable (Figures 2-5). Genesis density in regions such as Greenland, in the North Atlantic, and the southeastern Brazilian coast, in the South Atlantic, seem to be enhanced by the addition of short-lived cyclones included in the statistics. These regions are also highlighted when a smaller displacement threshold is applied (Figure 1). Crespo et al. (2020b) showed five genesis region in South America without the application of any displacement threshold, contrasting the three well-known cyclogenetic regions (Hoskins and Hodges, 2005; Reboita et al., 2010; Gramscianinov et al., 2019). The use of displacement threshold is necessary to avoid the inclusion of thermal and continental lows in the climatology, which may not develop into a cyclone.

Another source of discrepancies between the present and previous studies is the use of 1-hourly tracking, since most climatologies are constructed based on 6-hourly atmospheric fields. The improved time-resolution tracking can result in slight differences in genesis position, such as can be observed on the East South American coast. Despite the same tracking method and thresholds, this work present a higher genesis density in Uruguay and a smaller density in the Southeast Brazilian coast than Gramscianinov et al. (2019), which can be associated with the identification of cyclones at earlier lifecycle stages with the use of 1-hourly tracking, instead of 6-hourly. Gramscianinov et al. (2019) used an artificial orographic barrier to impose an Andes constraint to their tracking method, which could influence the genesis region position in their work.

Regarding the main differences between the two data sets, ERA5 presents 3.7% more cyclones than CFSR/CFSv2 (45.2 cyclones per year), which can be related to the higher

resolution of the former. The higher amount of cyclones in the ERA5 impacts the spatial distribution differences both in the North Atlantic and South Atlantic. The track density difference shows a homogeneous distribution in the major part of both domains and does not reveal a shift between the tracks of the two datasets. The direct relation between model resolution and the number of detected cyclones are indicated in many studies (e.g., Bengtsson et al., 2006). The impact of resolution is affected by the orography representation and small-scale processes important to genesis and growth. Therefore, the T42 filtering before the identification process and tracking does not completely exclude the effects of the resolution on the representation of cyclones in ERA5.

Cyclogenesis density differences show that CFSR/CFSv2 favors genesis off coast and above the ocean sector, which induce a bias in genesis region along East of the North American coast and Southwest of South American coast when compared to ERA5. This meridional shift in genesis regions may also be related to resolution, once the best representation of orography, land contrast and sea surface temperature can lead to early cyclone detection (e.g., Bengtsson et al., 2006) in the ERA5. However, the differences in genesis densities are evidence of differences in the track lengths between the two datasets. ERA5 presents cyclones that lived longer and travel further than CFSR/CFSv2 (Figure 7), which can be addressed to the inconsistency between forecast and analysis sequential time-steps. Abrupt changes in atmospheric patterns between the forecast and analysis time-step can interrupt a track, breaking a unique cyclone track into two. This continuity issue in CFSR/CFSv2 influences its genesis density, and also its stronger initial vorticity, since a broken track leads to a new track that starts in a more mature stage of the cyclone.

Cyclone annual mean and mean characteristics, such as displacement speed and initial vorticity are similar between the two datasets, and their differences are less than 1 standard deviation. Moreover, the track correspondence between the two datasets is high, being higher than 90% to the whole period. In Hodges et al. (2011), the differences between more recent datasets, ERA-Interim and CFSR, were smaller when compared to other older and coarser resolution reanalysis. Both ERA5 and CFSR/CFSv2 are considered to be high-resolution global products, and state of the art for analysis and reanalysis methodology.

The most pronounced difference is in the intensity distribution, which shows more intense cyclones in CFSR/CFSv2 than in ERA5. The CFS family present a tendency to represent more intense cyclones, winds and, consequently waves, as reported by several works (e.g., Hodges et al., 2011; Stopa and Cheung, 2014; Gramscianinov et al., 2020b). There are no significant difference between ERA5 and CFSR/CFSv2 when mean maximum wind speed is considered, but the differences increase in the higher percentiles of the distributions (Table 4). The 10-m wind components are diagnostic variables, and their computation depends on the different boundary layers models component of each dataset. Even so, these parameters are widely used in oceanography and ocean engineering studies and the evaluation of cyclone intensity by these fields is of great value.

This study shows that the differences between ERA5 and CFSR/CFSv2 are larger for the South Atlantic than North Atlantic. Other comparison studies found the same behavior (e.g., Hodges et al., 2003; 2011; Stoppa and Cheung, 2004). However, there is a decrease of discrepancies between ERA5 and the more recent CFSv2 when compared to CFSR, particularly in the South Atlantic Ocean. The decrease in differences between datasets in recent years reflects

the improvement of the models and increase in data availability as discussed by Hodges et al. (2010).

The storm tracks for ERA5 and CFSR/CFSv2 used to produce the climatologies presented in this work are available in <ftp://masterftp.iag.usp.br/EXWAV>. The provided product consists of the set of monthly tracks files that contain the positional information of cyclones.

5. Conclusions

This study has evaluated and compared the cyclone climatologies for ERA5 and CFSR/CFSv2 at middle and high latitudes. First, the performance of 1-hourly ERA5 and CFSR/CFSv2 tracking in reproducing the Atlantic storm tracks was analyzed regarding the past literature. Then, the two climatologies were compared to access the main differences between them regarding the basics of storm track characteristics.

The storm tracks are in good agreement with past studies, both to North Atlantic (e.g., Hoskins and Hodges, 2002; Trigo, 2006; Dacre and Gray, 2009; Grise et al., 2013), and South Atlantic Oceans (e.g., Gan and Rao, 1991; Mendes et al., 2010; Reboita et al., 2010; Gramscianinov et al., 2019; Crespo et al., 2020b). The main North Atlantic and South Atlantic storm track characteristics, such as the spiral pattern poleward, seasonal variability, and latitudinal range are represented, as well as the well-known genesis regions within these ocean basins. The use of hourly fields brought benefits to the tracking, particularly in areas with complex terrains, such as the lee of Andes Cordillera in the South America, and East of Greenland in the North Atlantic.

Differences between datasets showed that ERA5 has 3.7% more cyclones than CFSR/CFSv2, which can be related to the finer resolution (e.g., Bengtsson et al., 2006). However, cyclone

annual mean and mean characteristics (e.g., displacement speed) are similar between the two datasets, and 90% of the tracks correspond between them. An important difference between ERA5 and CFSR/CFSv2 are the shifts in genesis density along the eastern coast, both in North and South America, which can be an indication of resolution impact in cyclone development in regions with complex orography, and temperature gradient. Furthermore, continuity issues in CFSR/CFSv2 due to jumps that might occur where forecast time-steps change to analysis time-steps can lead to broken tracks, and thus, differences between the two datasets, particularly related to genesis statistics and cyclone duration lifecycle.

Other relevant differences between ERA5 and CFSR/CFSv2 are the intensity distributions, particularly in the higher percentile of maximum 10-m wind speed. The CFSR/CFSv2 dataset presents more intense cyclones than ERA5 and this behavior persists even when CFSR and CFSv2 were evaluated separately. Other studies have already reported the ability of CFSR (Hodges et al., 2011; Stopa and Cheung, 2014) and CFSv2 (e.g., Gramscianinov et al., 2020b) to represent more extreme wind speed values. It is remarkable that in most of the analyses performed in this work, the differences between datasets decrease when CFSv2 period is analyzed separately, revealing rather a bias correction in the operational version of CFS or an increase of available data and improvement of data assimilation method. In fact, the discrepancies reduction is more pronounced in the South Atlantic, which reinforces the role of data assimilation process in the convergence of the two datasets (e.g., Hodges et al., 2011; Stopa and Cheung, 2014).

Acknowledgments

This work is part of the project “Extreme wind and wave modeling and statistics in the Atlantic Ocean” (EXWAV) funded by the Portuguese Foundation for Science and Technology (Fundação para a Ciência e Tecnologia – FCT) under contract PTDC/EAM-OCE/31325/2017 RD0504, and by the São Paulo Research Foundation (FAPESP) grant #2018/08057-5. C.B.G. holds a FAPESP post-doc scholarship grant #2020/01416-0. The authors would like to acknowledge the NCEP and ECMWF for providing the atmospheric and wave data for the study. The ERA5 products were generated using Copernicus Climate Change Service Information [2019]. This study used the high-performance computing resources of the SDumont supercomputer (<http://sdumont.lncc.br>), which is provided by the National Laboratory for Scientific Computing (LNCC/MCTI, Brazil).

References

- Bakhtyar, R., Orton, P.M., Marsooli, R., Miller, J.K., 2018. Rapid wave modeling of severe historical extratropical cyclones off the Northeastern United States. *Ocean Eng.* 159, 315–332. <https://doi.org/10.1016/j.oceaneng.2018.04.037>
- Belmonte Rivas, M., Stoffelen, A., 2019. Characterizing ERA-Interim and ERA5 surface wind biases using ASCAT. *Ocean Sci.* 15, 831–852. <https://doi.org/10.5194/os-15-831-2019>
- Bengtsson, L., Hodges, K.I., Keenlyside, N., 2009. Will extratropical storms intensify in a warmer climate? *J. Clim.* 22, 2276–2301. <https://doi.org/10.1175/2008JCLI2678.1>
- Bengtsson, L., Hodges, K.I., Roeckner, E., 2006. Storm tracks and climate change. *J. Clim.* 19, 3518–3543. <https://doi.org/10.1175/JCLI3815.1>

498 Booth, J.F., Rieder, H.E., Kushnir, Y., 2016. Comparing hurricane and extratropical storm surge
 499 for the Mid-Atlantic and Northeast Coast of the United States for 1979-2013. *Environ. Res.*
 500 *Lett.* 11(9). 10.1088/1748-9326/11/9/094004

501 Campos, R.M., Guedes Soares, C., 2016. Comparison and Assessment of Three Wave Hindcasts
 502 in the North Atlantic Ocean. *J. Oper. Oceanogr.* 9(1):26-44.
 503 <https://doi.org/10.1080/1755876X.2016.1200249>

504 Campos, R.M., Guedes Soares, C., 2017. Assessment of Three Wind Reanalysis in the North
 505 Atlantic Ocean. *J. Oper. Oceanogr.* 10(1):30-44.
 506 <https://doi.org/10.1080/1755876X.2016.1253328>

507 Campos, R.M., Alves, J.H.G.M., Guedes Soares, C., Guimaraes, L.G., Parente, C.E., 2018.
 508 Extreme wind-wave modeling and analysis in the South Atlantic Ocean. *Ocean Model.* 124,
 509 75–93. <https://doi.org/10.1016/j.ocemod.2018.02.002>

510 Campos, R.M., Guedes Soares, C., Alves, J.H.G.M., Parente, C.E., Guimaraes, L.G., 2019.
 511 Regional long-term extreme wave analysis using hindcast data from the South Atlantic
 512 Ocean. *Ocean Eng.* 179, 202–212. <https://doi.org/10.1016/j.oceaneng.2019.03.023>

513 Chelton, D. B., Schlax, M. G., Freilich, M. H., Milliff, R. F., 2004. Satellite measurements reveal
 514 persistent small-scale features in ocean winds. *Science* 303, 978–983,
 515 <https://doi.org/10.1126/science.1091901>

516 Colle, B.A., Rojowsky, K., Buonaito, F., 2010. New York city storm surges: Climatology and an
 517 analysis of the wind and cyclone evolution. *J. Appl. Meteorol. Climatol.* 49(1): 85–100.
 518 10.1175/2009JAMC2189.1

519 Copernicus Climate Change Service (C3S) 2017. ERA5: Fifth generation of ECMWF
 520 atmospheric reanalyses of the global climate. Copernicus Climate Change Service Climate
 521 Data Store (CDS), July, 2019.

522 Crespo, N.M.; da Rocha, R.P.; De Jesus, E.M., 2020a. Cyclones density and characteristics in
 523 different reanalyses dataset over South America. In: EGU General Assembly 2020, Online, 4-
 524 8 May 2020, EGU2020-11316. <https://doi.org/10.5194/egusphere-egu2020-11316>

525 Crespo, N.M., da Rocha, R.P., Sprenger, M., Wernli, H., 2020b. A Potential Vorticity
 526 Perspective on Cyclogenesis over Center-Eastern South America. *Int. J. Climatol.* 1-16.
 527 <https://doi.org/10.1002/joc.6644>

528 Dacre, H.F., Gray, S.L., 2009. The spatial distribution and evolution characteristics of North
 529 Atlantic cyclones. *Mon. Weather Rev.* 137, 99–115.
 530 <https://doi.org/10.1175/2008MWR2491.1>

531 Dacre, H.F., Hawcroft, M.K., Stringer, M.A., Hodges, K.I., 2012. An extratropical cyclone atlas
 532 a tool for illustrating cyclone structure and evolution characteristics. *Bull. Am. Meteorol. Soc.*
 533 93, 1497–1502. <https://doi.org/10.1175/BAMS-D-11-00164.1>

534 Evans, J. L., Braun, A., 2012. A Climatology of Subtropical Cyclones in the South Atlantic. *J.*
 535 *Climate* 25, 7328–7340, <https://doi.org/10.1175/JCLI-D-11-00212.1>.

536 Gan, M.A., Rao, V.B., 1991. Surface Cyclogenesis over South America. *Mon. Weather Rev.*
 537 119, 1293–1302. [https://doi.org/10.1175/1520-0493\(1991\)119<1293:SCOSA>2.0.CO;2](https://doi.org/10.1175/1520-0493(1991)119<1293:SCOSA>2.0.CO;2)

538 Gozzo, L.F., da Rocha, R.P., Reboita, M.S., Sugahara, S., 2014. Subtropical cyclones over the
 539 southwestern South Atlantic: Climatological aspects and case study. *J. Clim.* 27, 8543–8562.
 540 <https://doi.org/10.1175/JCLI-D-14-00149.1>

541 Gramscianinov, C.B., Campos, R.M., Guedes Soares, C., Camargo, R., 2020a. Extreme waves
 542 generated by cyclonic winds in the western portion of the South Atlantic Ocean. *Ocean Eng.*
 543 213: 107745. <https://doi.org/10.1016/j.oceaneng.2020.107745>
 544 Gramscianinov, Campos, R.M., Guedes Soares, C., Camargo, R., 2020b. Comparison between
 545 ERA5 and CFS datasets of extratropical cyclones associated with extreme wave events in the
 546 Atlantic Ocean. *Proceedings of the ASME 2020 29th International Conference on Offshore*
 547 *Mechanics and Arctic Engineering*, Online, 3-7 August, 2020, ASME.
 548 Gramscianinov, C.B., Hodges, K.I., Camargo, R., 2019. The properties and genesis environments
 549 of South Atlantic cyclones. *Clim. Dyn.* 53, 4115–4140. [https://doi.org/10.1007/s00382-019-](https://doi.org/10.1007/s00382-019-04778-1)
 550 [04778-1](https://doi.org/10.1007/s00382-019-04778-1)
 551 Grise, K.M., Son, S.W., Gyakum, J.R., 2013. Intraseasonal and interannual variability in north
 552 american storm tracks and its relationship to equatorial pacific variability. *Mon. Weather Rev.*
 553 141, 3610–3625. <https://doi.org/10.1175/MWR-D-12-00322.1>
 554 Guishard, M.P., Evans, J.L., Hart, R.E., 2009. Atlantic subtropical storms. Part II: Climatology.
 555 *J. Clim.* 22, 3574 – 3594. <https://doi.org/10.1175/2008JCLI2346.1>
 556 Hersbach, H., Dee, D., 2016. ERA5 reanalysis is in production, *ECMWF Newsletter* 147,
 557 ECMWF, Reading, UK, 2016.
 558 Hersbach, H., Bell, B., Berrisford, P., Horányi, A., Sabater, J.M., Nicolas, J., Radu, R., Schepers,
 559 D., Simmons, A., Soci, C., Dee, D., 2018. Global reanalysis: goodbye ERA-Interim, hello
 560 ERA5. *ECMWF Newsl.* 17–24. <https://doi.org/10.21957/vf291hehd7>
 561 Hodges, K.I., 1994. A General Method for Tracking Analysis and Its Application to
 562 Meteorological Data. *Mon. Weather Rev.* 122, 2573–2586. [https://doi.org/10.1175/1520-](https://doi.org/10.1175/1520-0493(1994)122<2573:AGMFTA>2.0.CO;2)
 563 [0493\(1994\)122<2573:AGMFTA>2.0.CO;2](https://doi.org/10.1175/1520-0493(1994)122<2573:AGMFTA>2.0.CO;2)

564 Hodges, K.I., 1995. Feature Tracking on the Unit Sphere. *Mon. Weather Rev.* 123, 3458–3465.
 565 [https://doi.org/10.1175/1520-0493\(1995\)123<3458:FTOTUS>2.0.CO;2](https://doi.org/10.1175/1520-0493(1995)123<3458:FTOTUS>2.0.CO;2)
 566 Hodges, K.I., 1996. Spherical Nonparametric Estimators Applied to the UGAMP Model
 567 Integration for AMIP. *Mon. Weather Rev.* 124, 2914–2932. [https://doi.org/10.1175/1520-](https://doi.org/10.1175/1520-0493(1996)124<2914:SNEATT>2.0.CO;2)
 568 [0493\(1996\)124<2914:SNEATT>2.0.CO;2](https://doi.org/10.1175/1520-0493(1996)124<2914:SNEATT>2.0.CO;2)
 569 Hodges, K.I., 1999. Adaptive constraints for feature tracking. *Mon. Weather. Rev.*, 127, 1362–
 570 1373. [https://doi.org/10.1175/1520-0493\(1999\)127<1362:ACFFT>2.0.CO;2](https://doi.org/10.1175/1520-0493(1999)127<1362:ACFFT>2.0.CO;2)
 571 Hodges, K.I., 2008: Confidence intervals and significance tests for spherical data derived from
 572 feature tracking. *Mon. Weather Rev.*, 136, 1758–1777.
 573 <https://doi.org/10.1175/2007MWR2299.1>
 574 Hodges, K.I., Hoskins, B.J., Boyle, J., Thorncroft, C., 2003. A Comparison of Recent Reanalysis
 575 Datasets Using Objective Feature Tracking: Storm Tracks and Tropical Easterly Waves. *Mon.*
 576 *Weather Rev.* 131, 2012–2037. [https://doi.org/10.1175/1520-](https://doi.org/10.1175/1520-0493(2003)131<2012:ACORRD>2.0.CO;2)
 577 [0493\(2003\)131<2012:ACORRD>2.0.CO;2](https://doi.org/10.1175/1520-0493(2003)131<2012:ACORRD>2.0.CO;2)
 578 Hodges, K.I., Lee, R.W., Bengtsson, L., 2011. A comparison of extratropical cyclones in recent
 579 reanalyses ERA-Interim, NASA MERRA, NCEP CFSR, and JRA-25. *J Clim* 24:4888–4906.
 580 <https://doi.org/10.1175/2011JCLI4097.1>
 581 Hoskins, B.J., Hodges, K.I., 2002. New Perspectives on the Northern Hemisphere Winter Storm
 582 Tracks. *J. Atmos. Sci.* 59, 1041–1061. [https://doi.org/10.1175/1520-](https://doi.org/10.1175/1520-0469(2002)059<1041:NPOTNH>2.0.CO;2)
 583 [0469\(2002\)059<1041:NPOTNH>2.0.CO;2](https://doi.org/10.1175/1520-0469(2002)059<1041:NPOTNH>2.0.CO;2)
 584 Hoskins, B.J., Hodges, K.I., 2005. A New Perspective on Southern Hemisphere Storm Tracks. *J.*
 585 *Clim.* 18, 4108–4129. <https://doi.org/10.1175/JCLI3570.1>

586 Jones, D.A., Simmonds, I., 1993. A climatology of Southern Hemisphere extratropical cyclones.
 587 Climate Dyn. 9, 131–145. <https://doi.org/10.1007/BF00209750>
 588 Kalnay, E., Kanamitsu, M., Kistler, R., Collins, W., Deaven, D., Gandin, L., Iredell, M., Saha,
 589 S., White, G., Woollen, J., Zhu, Y., Chelliah, M., Ebisuzaki, W., Higgins, W., Janowiak, J.,
 590 Mo, K.C., Ropelewski, C., Wang, J., Leetmaa, A., Reynolds, R., Jenne, R., Joseph, D., 1996.
 591 The NCEP/NCAR 40-Year Reanalysis Project. Bull. Amer. Meteor. Soc., 77, 437–472.
 592 [https://doi.org/10.1175/1520-0477\(1996\)077<0437:TNYRP>2.0.CO;2](https://doi.org/10.1175/1520-0477(1996)077<0437:TNYRP>2.0.CO;2)
 593 Kumar, V.S., Mandal, S., Kumar, K.A., 2003. Estimation of wind speed and wave height during
 594 cyclones. Ocean Eng. 30, 2239–2253. [https://doi.org/10.1016/S0029-8018\(03\)00076-3](https://doi.org/10.1016/S0029-8018(03)00076-3)
 595 Mattioli, M., De Masi, G., Drago, M., 2019. Evaluating extreme cyclonic sea states. Ocean Eng.
 596 194, 106639. <https://doi.org/10.1016/j.oceaneng.2019.106639>
 597 Mendes, D., Souza, E.P., Marengo, J.A., Mendes, M.C.D., 2010. Climatology of extratropical
 598 cyclones over the South American-southern oceans sector. Theor. Appl. Climatol. 100, 239–
 599 250. <https://doi.org/10.1007/s00704-009-0161-6>
 600 Murray, R.J., Simmonds, I., 1991a. A numerical scheme for tracking cyclone centres from digital
 601 data Part I: development and operation of the scheme. Aust. Meteorol. Mag. 39, 155–166.
 602 Murray, R.J., Simmonds, I., 1991b. A numerical scheme for tracking cyclone centres from
 603 digital data. Part II: application to January and July general circulation model simulations.
 604 Aust. Meteorol. Mag. 39, 155–166.
 605 Olauson, J., 2018. ERA5: The new champion of wind power modelling? Renew. Energy 126,
 606 322–331. <https://doi.org/10.1016/j.renene.2018.03.056>
 607 Onogi, K., Tsutsui, J., Koide, H., Sakamoto, M., Kobayashi, S., Hatsushika, H., Matsumoto, T.,
 608 Yamazaki, N., Kamahori, H., Takahashi, K., Kadokura, S., Wada, K., Kato, K., Oyama, R.,

609 Ose, T., Mannoji, N., Taira, R., 2007. The JRA-25 Reanalysis. *J. Meteorol. Soc. Japan. Ser. II*
 610 85, 369–432. <https://doi.org/10.2151/jmsj.85.369>
 611 Parker, W.S., 2016. Reanalyses and observations: What’s the Difference? *Bull. Am. Meteorol.*
 612 *Soc.* 97, 1565–1572. <https://doi.org/10.1175/BAMS-D-14-00226.1>
 613 Pinto, J.G., Spanghel, T., Ulbrich, U., Speth, P., 2005. Sensitivities of a cyclone detection and
 614 tracking algorithm: Individual tracks and climatology. *Meteorol. Zeitschrift* 14, 823–838.
 615 <https://doi.org/10.1127/0941-2948/2005/0068>
 616 Ponce De León, S., Guedes Soares, C., 2012. Distribution of winter wave spectral peaks in the
 617 seas around Norway. *Ocean Eng.* 50, 63–71. <https://doi.org/10.1016/j.oceaneng.2012.05.005>
 618 Raible, C.C., Della-Marta, P.M., Schwierz, C., Wernli, H., Blender, R., 2008. Northern
 619 Hemisphere Extratropical Cyclones: A Comparison of Detection and Tracking Methods and
 620 Different Reanalyses. *Mon. Weather Rev.* 136, 880–897.
 621 <https://doi.org/10.1175/2007MWR2143.1>
 622 Reboita, M.S., da Rocha, R.P., Ambrizzi, T., Sugahara, S., 2010. South Atlantic Ocean
 623 cyclogenesis climatology simulated by regional climate model (RegCM3). *Clim. Dyn.* 35,
 624 1331–1347. <https://doi.org/10.1007/s00382-009-0668-7>
 625 Reboita, M.S., da Rocha, R.P., de Souza, M.R., Llopart, M., 2018. Extratropical cyclones over
 626 the southwestern South Atlantic Ocean: HadGEM2-ES and RegCM4 projections. *Int. J.*
 627 *Climatol.* 38, 2866–2879. <https://doi.org/10.1002/joc.5468>
 628 Rienecker, M.M., Suarez, M.J., Gelaro, R., Todling, R., Bacmeister, J., Liu, E., Bosilovich,
 629 M.G., Schubert, S.D., Takacs, L., Kim, G., Bloom, S., Chen, J., Collins, D., Conaty, A., da
 630 Silva, A., Gu, W., Joiner, J., Koster, R.D., Lucchesi, R., Molod, A., Owens, T., Pawson, S.,
 631 Pegion, P., Redder, C.R., Reichle, R., Robertson, F.R., Ruddick, A.G., Sienkiewicz, M..

632 Woollen, J., 2011. MERRA: NASA's Modern-Era Retrospective Analysis for Research and
633 Applications. *J. Climate*, 24, 3624–3648

634 Saha, S., Moorthi, S., Pan, H., Wu, X., Wang, J., Nadiga, S., Tripp, P., Kistler, R., Woollen, J.,
635 Behringer, D., Liu, H., Stokes, D., Grumbine, R., Gayno, G., Wang, J., Hou, Y., Chuang, H.,
636 Juang, H.H., Sela, J., Iredell, M., Treadon, R., Kleist, D., Delst, P. Van, Keyser, D., Derber,
637 J., Ek, M., Meng, J., Wei, H., Yang, R., Lord, S., Dool, H. van den, Kumar, A., Wang, W.,
638 Long, C., Chelliah, M., Xue, Y., Huang, B., Schemm, J., Ebisuzaki, W., Lin, R., Xie, P.,
639 Chen, M., Zhou, S., Higgins, W., Zou, C., Liu, Q., Chen, Y., Han, Y., Cucurull, L., Reynolds,
640 R.W., Rutledge, G., Goldberg, M., 2010. The NCEP Climate Forecast System Reanalysis.
641 *Bull. Amer. Meteor. Soc.*, 91, 1015–1058. <https://doi.org/10.1175/2010BAMS3001.1>

642 Saha, S., S. Moorthi, S., Wu, X., Wang, J., Nadiga, S., Tripp, P., Behringer, D., Hou, Y., Chuang,
643 H., Iredell, M., Ek, M., Meng, J., Yang, R., Mendez, M.P., Dool, H. van den, Zhang, Q.,
644 Wang, W., Chen, M., Becker, E., 2014. The NCEP Climate Forecast System Version 2. *J.*
645 *Climate*, 27, 2185–2208. <https://doi.org/10.1175/JCLI-D-12-00823.1>

646 Sebastian, M., Behera, M.R., Murty P.L.N., 2019. Storm surge hydrodynamics at a concave
647 coast due to varying approach angles of cyclone. *Ocean. Eng.* 191.
648 <https://doi.org/10.1016/j.oceaneng.2019.106437>

649 Simmonds, I., Keay, K., 2000. Mean southern hemisphere extratropical cyclone behavior in the
650 40-year NCEP-NCAR reanalysis. *J. Clim.* 13, 873–885. [https://doi.org/10.1175/1520-](https://doi.org/10.1175/1520-0442(2000)013<0873:MSHECB>2.0.CO;2)
651 [0442\(2000\)013<0873:MSHECB>2.0.CO;2](https://doi.org/10.1175/1520-0442(2000)013<0873:MSHECB>2.0.CO;2)

652 Simmonds, I., Keay, K., 2000. Mean southern hemisphere extratropical cyclone behavior in the
653 40-year NCEP-NCAR reanalysis. *J. Clim.* 13, 873–885. [https://doi.org/10.1175/1520-](https://doi.org/10.1175/1520-0442(2000)013<0873:MSHECB>2.0.CO;2)
654 [0442\(2000\)013<0873:MSHECB>2.0.CO;2](https://doi.org/10.1175/1520-0442(2000)013<0873:MSHECB>2.0.CO;2)

Simmons, A., Uppala, S., Dee, D., Kobayashi, S., 2007. ERA-Interim: New ECMWF reanalysis products from 1989 onwards. *ECMWF Newsletter* 110, ECMWF, Reading, UK, 25–35.

Sinclair, M.R., 1994. An objective cyclone climatology for the Southern Hemisphere. *Mon. Wea. Rev.*, 122, 2239–2256.

Sinclair, M.R., 1997. Objective Identification of Cyclones and Their Circulation Intensity, and Climatology. *Weather Forecast.* 12, 595–612. [https://doi.org/10.1175/1520-0434\(1997\)012<0595:OIOCAT>2.0.CO;2](https://doi.org/10.1175/1520-0434(1997)012<0595:OIOCAT>2.0.CO;2)

Stopa, J.E., Cheung, K.F., 2014. Intercomparison of wind and wave data from the ECMWF Reanalysis Interim and the NCEP Climate Forecast System Reanalysis. *Ocean Model.* 75, 65–83.

Trigo, I.F., 2006. Climatology and interannual variability of storm-tracks in the Euro-Atlantic sector: A comparison between ERA-40 and NCEP/NCAR reanalyses. *Clim. Dyn.* 26, 127–143. <https://doi.org/10.1007/s00382-005-0065-9>

Vettor, R., Guedes Soares, C., 2016. Rough weather avoidance effect on the wave climate experienced by oceangoing vessels. *Appl. Ocean Res.* 59, 606–615. <https://doi.org/10.1016/j.apor.2016.06.004>

Vettor, R., Guedes Soares, C., 2017. Characterization of the expected weather conditions in the main European coastal traffic routes. *Ocean Eng.* 140, 244–257. <https://doi.org/10.1016/j.oceaneng.2017.05.027>

Tables

Table 1. Mean number of cyclones tracked in ERA5 and CFSR/CFSv2 between 1979 and 2019, annual and seasonal mean. The mean are also computed for CFSR (1979-March/2011) and CFSv2 (April/2011-2019) alone. All cyclones that pass within the extratropical latitudes of the South Atlantic (SA; 85°S-25°S, 75°W-20°E) and North Atlantic (NA; 85°N-25°N, 65°W-0°E) Oceans were considered.

		1979-2019				
		Annual	DJF	MAM	JJA	SON
NA	ERA5	551.0 ± 23.6	155.8 ± 9.7	140.9 ± 10.6	117.5 ± 8.3	136.7 ± 9.1
	CFSR/CFSv2	538.7 ± 21.2	152.9 ± 8.1	135.2 ± 11.3	118.0 ± 7.9	132.7 ± 8.8
SA	ERA5	730.9 ± 21.4	158.2 ± 10.0	184.8 ± 11.5	201.9 ± 11.7	186.0 ± 9.9
	CFSR/CFSv2	698.0 ± 19.7	154.2 ± 9.6	177.1 ± 10.6	189.3 ± 10.2	177.4 ± 10.0
		1979-2011				
		Annual	DJF	MAM	JJA	SON
NA	ERA5	537.8 ± 72.5	154.4 ± 14.8	137.7 ± 16.4	117.5 ± 8.7	135.8 ± 8.9
	CFSR	525.2 ± 69.9	151.7 ± 12.9	131.7 ± 16.9	117.5 ± 7.3	131.8 ± 8.4
SA	ERA5	709.2 ± 100.4	155.0 ± 14.1	180.9 ± 24.5	200.3 ± 11.8	184.6 ± 10.6
	CFSR	678.7 ± 97.5	151.5 ± 14.4	174.3 ± 24.3	187.8 ± 10.1	176.2 ± 10.4
		2011-2019				
		Annual	DJF	MAM	JJA	SON
NA	ERA5	538.1 ± 52.9	143.8 ± 36.6	137.2 ± 18.6	117.6 ± 7.0	139.6 ± 9.4
	CFSv2	528.6 ± 54.0	140.0 ± 35.6	133.1 ± 16.6	119.8 ± 10.0	135.7 ± 10.0
SA	ERA5	729.3 ± 57.9	152.4 ± 33.9	178.4 ± 22.3	207.7 ± 9.8	190.8 ± 5.1
	CFSv2	691.0 ± 61.2	147.1 ± 30.9	167.8 ± 21.6	194.6 ± 9.5	181.6 ± 7.6

Table 2. Mean characteristics of cyclones for ERA5 and CFSR/CFSv2 (1979-2019), and computed for CFSR (1979-March/2011) and CFSv2 (April/2011-2019) separately. Initial vorticity is the filtered relative vorticity at the time of genesis, and is scaled by -1 in South Atlantic. Displacement is computed using the first and the last track point. All cyclones that pass within the extratropical latitudes of the South Atlantic (SA; 85°S-25°S, 75°W-20°E) and North Atlantic (NA; 85°N-25°N, 65°W-0°E) Oceans were considered.

1979 - 2019					
		Initial vorticity (CVU)	Lifetime (days)	Displacement (m)	Speed (km h ⁻¹)
NA	ERA5	2.7 ± 1.4	4.4 ± 3.0	2928.5 ± 1582.2	9.6 ± 4.7
	CFSR/CFSv2	2.8 ± 1.5	4.0 ± 2.6	2767.8 ± 1467.6	9.8 ± 4.6
SA	ERA5	2.9 ± 1.5	3.9 ± 2.6	3712.0 ± 2157.9	13.2 ± 5.3
	CFSR/CFSv2	3.2 ± 1.6	3.3 ± 2.1	3228.3 ± 1855.6	13.3 ± 5.3
1979 - 2011					
		Initial vorticity (CVU)	Lifetime (days)	Displacement (m)	Speed (km h ⁻¹)
NA	ERA5	2.7 ± 1.4	4.4 ± 2.9	2919.2 ± 1569.4	9.6 ± 4.6
	CFSR	2.9 ± 1.5	4.0 ± 2.6	2750.6 ± 1452.6	9.8 ± 4.6
SA	ERA5	2.9 ± 1.5	3.9 ± 2.6	3688.0 ± 2146.9	13.2 ± 5.3
	CFSR	3.3 ± 1.6	3.2 ± 2.1	3155.5 ± 1799.8	13.3 ± 5.3
2011 - 2019					
		Initial vorticity (CVU)	Lifetime (days)	Displacement (m)	Speed (km h ⁻¹)
NA	ERA5	2.7 ± 1.5	4.5 ± 3.1	2962.5 ± 1628.0	9.6 ± 4.8
	CFSv2	2.8 ± 1.6	4.1 ± 2.7	2830.7 ± 1519.6	9.8 ± 4.7
SA	ERA5	3.0 ± 1.5	4.0 ± 2.7	3797.7 ± 2194.7	13.3 ± 5.4
	CFSv2	3.2 ± 1.6	3.6 ± 2.3	3490.3 ± 2022.5	13.4 ± 5.3

Table 3. Percentage of the number of matched tracks for ERA5 and CFSR/CFSv2 (1979-2019), CFSR (1979-March/2011), and CFSv2 (April/2011-2019). Similar tracks are obtained in DJF for the North Atlantic (NA), and JJA for the South Atlantic (SA) Oceans.

		1979 - 2019	1979 - 2011	2011 - 2019
NA	ERA5	92.7%	91.9%	87.1%
	CFSR/CFSv2	96.0%	94.9%	91.1%
SA	ERA5	93.1%	91.8%	89.2%
	CFSR/CFSv2	96.5%	95.4%	91.8%

698 **Table 4.** Mean maximum 10-m wind speed (m s^{-1}) and percentiles of cyclones for ERA5 and
699 CFSR/CFSv2 (1979-2019) in DJF for the North Atlantic (NA), and JJA for the South Atlantic (SA)
700 Oceans. Matched cyclones are identical storms find in both datasets.

		ERA5				CFSR/CFSv2			
		mean	50%	90%	95%	mean	50%	90%	95%
NA	all	21.4 ± 5.1	21.1	28.2	30.1	23.9 ± 6.4	23.7	32.5	35.0
	matched	21.5 ± 5.1	21.2	28.3	30.2	24.0 ± 6.4	23.8	32.6	35.0
SA	all	21.2 ± 4.8	21.0	27.3	29.3	23.4 ± 4.8	23.3	30.2	32.1
	matched	21.2 ± 4.8	21.0	27.4	29.3	23.4 ± 5.3	23.4	30.2	32.2

701

Figures

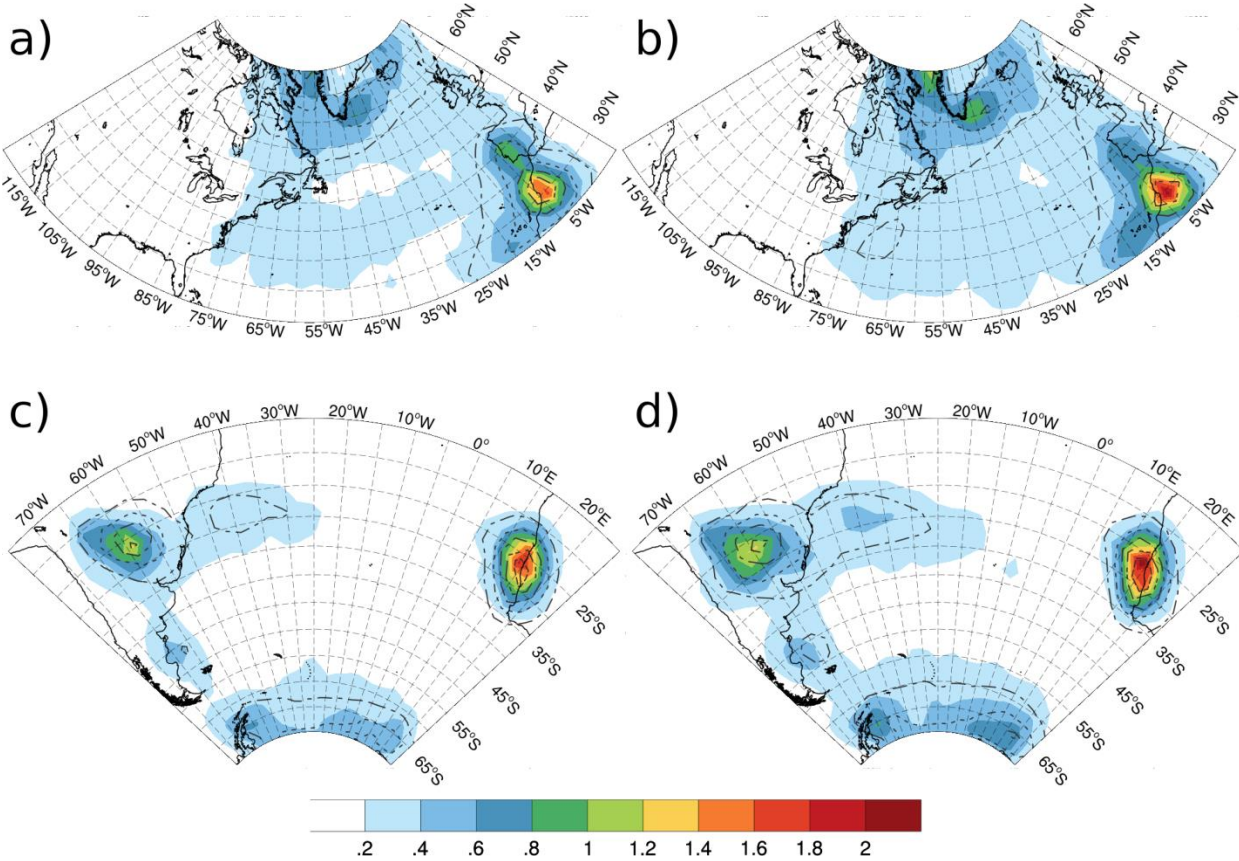


Figure 1. Genesis (shaded) and track (contour) densities computed for cyclones that last at least 24 hour and travel less than 1000 km for the (a) North Atlantic in ERA5 and (b) CFSR/CFSv2, and (c) South Atlantic in ERA5 and (d) CFSR/CFSv2. The density unit is cyclones/track per month per area, where the unit area is equivalent to a 5° spherical cap (10^6 km²). The track density contour are with contour interval 1 track per month per area, and the densities are calculated for 1979-2019.

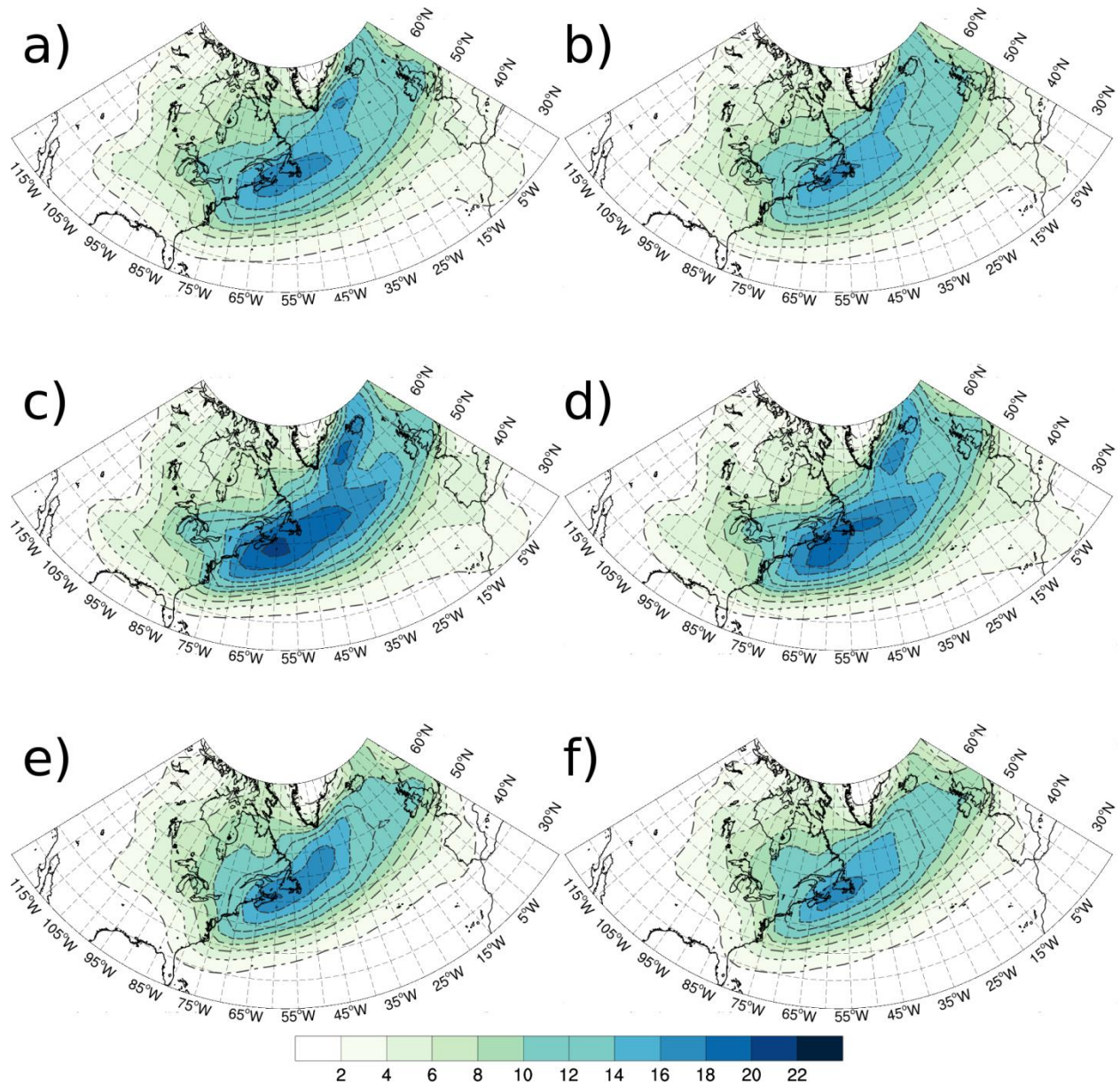


Figure 2. Track densities computed for the North Atlantic in (a,c,e) ERA5 and (b,d,f) CFSR/CFSv2, considering (a,b) all period (1979-2019), (c,d) DJF, and (e,f) JJA. The density unit is track per month per area, where the unit area is equivalent to a 5° spherical cap (10^6 km^2). The contour interval is 2 tracks per month per area.

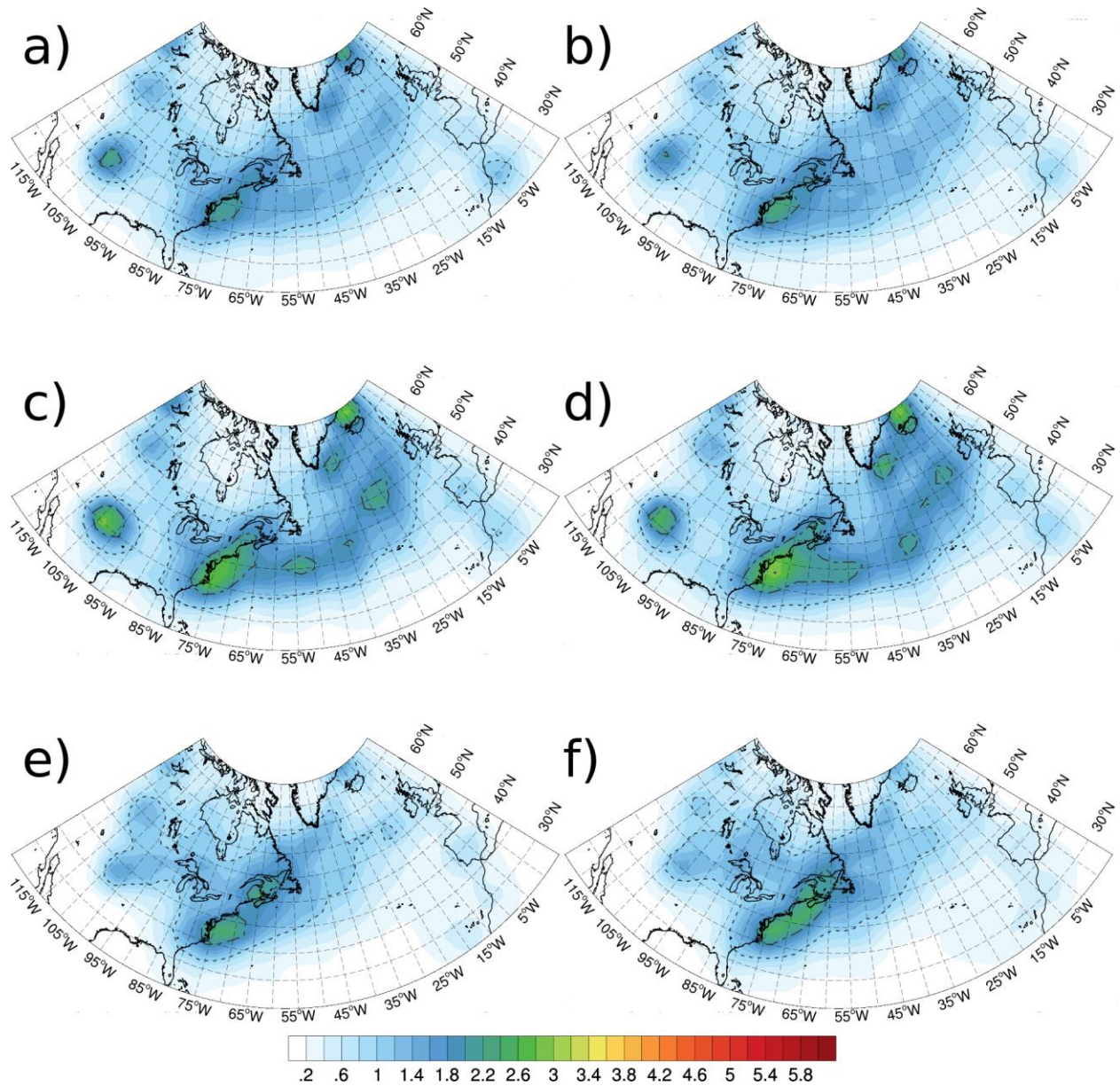


Figure 3. Genesis densities computed for the North Atlantic in (a,c,e) ERA5 and (b,d,f) CFSR/CFSv2, considering (a,b) all period (1979-2019), (c,d) DJF, and (e,f) JJA. The density unit is genesis per month per area, where the unit area is equivalent to a 5° spherical cap (10^6 km^2). The contour interval is 1 genesis per month per area.

715

716

717

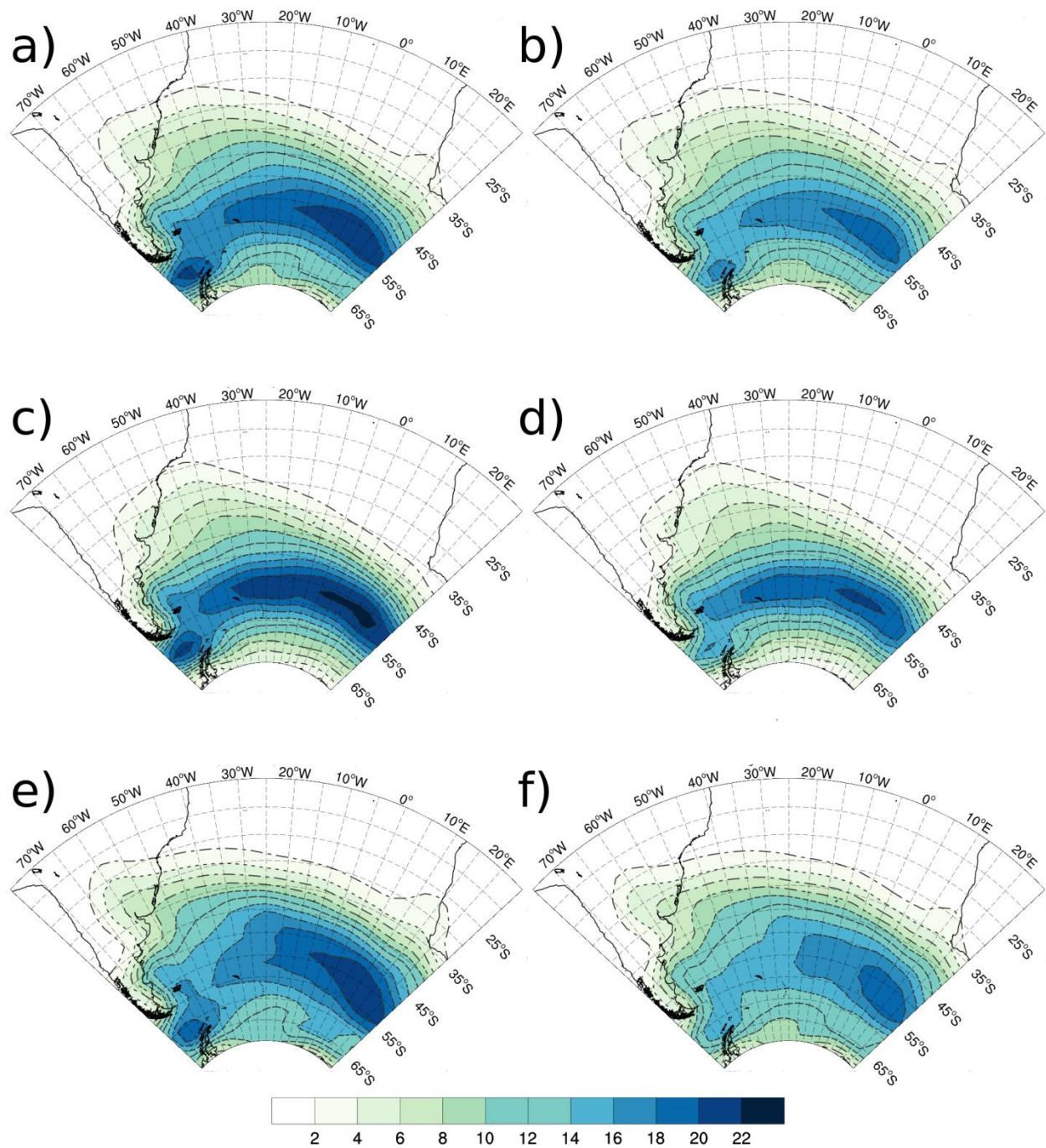


Figure 4. Track densities computed for the South Atlantic in (a,c,e) ERA5 and (b,d,f) CFSR/CFSv2, considering (a,b) all period (1979-2019), (c,d) DJF, and (e,f) JJA. The density unit is track per month per area, where the unit area is equivalent to a 5° spherical cap (10^6 km^2). The contour interval is 2 tracks per month per area.

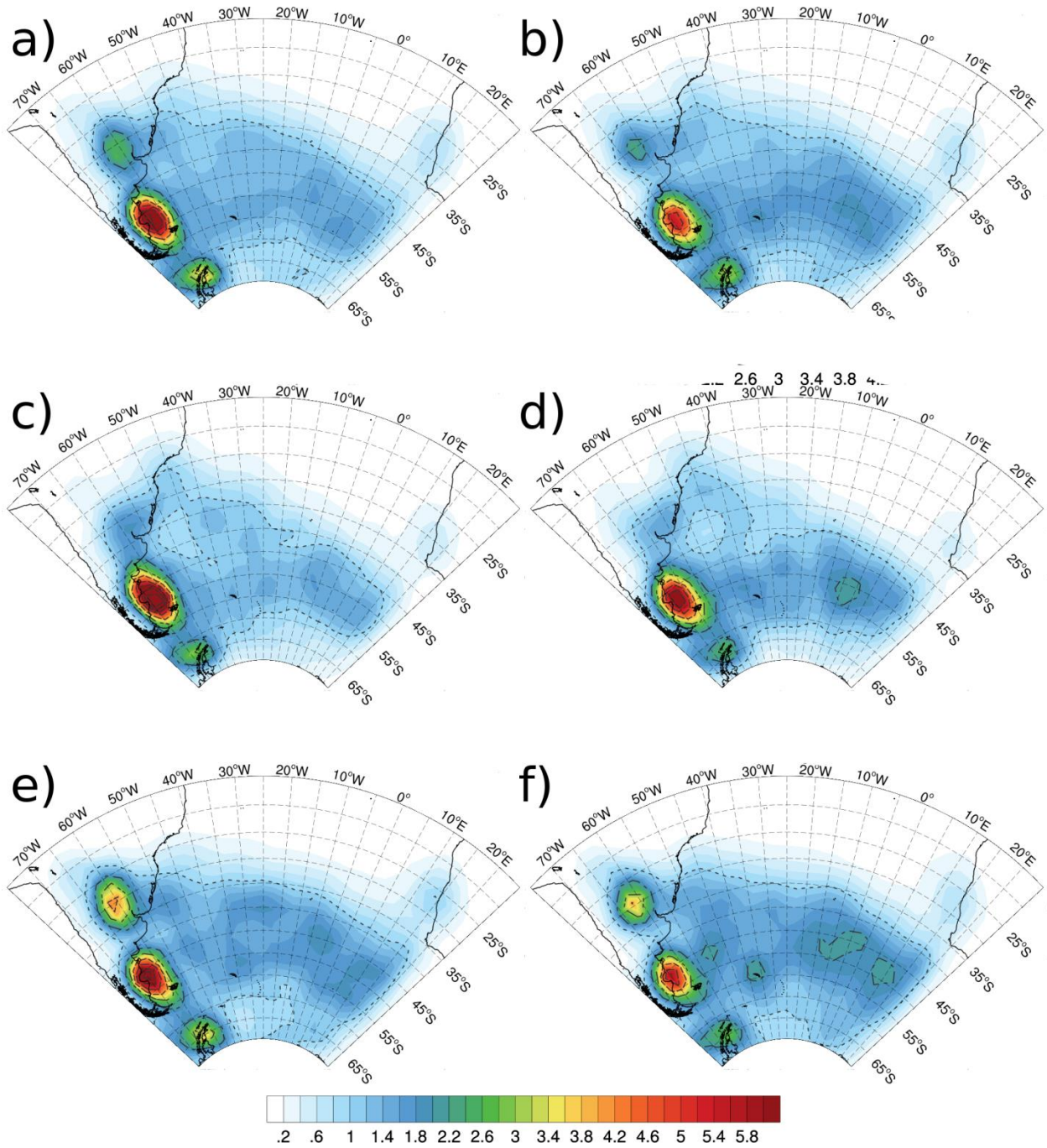


Figure 5. Genesis densities computed for the South Atlantic in (a,c,e) ERA5 and (b,d,f) CFSR/CFSv2, considering (a,b) all period (1979-2019), (c,d) DJF, and (e,f) JJA. The density unit is genesis per month per area, where the unit area is equivalent to a 5° spherical cap (10^6 km^2). The contour interval is 1 genesis per month per area.

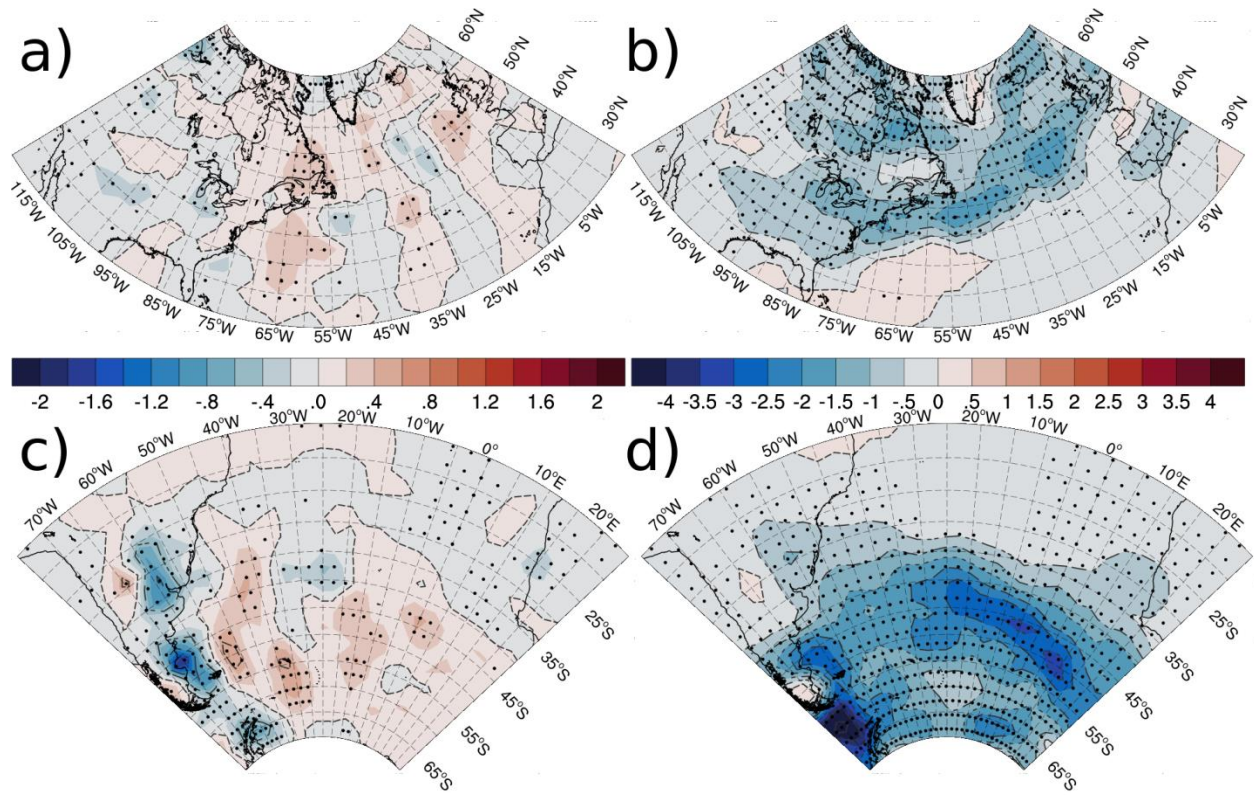


Figure 6. Densities differences in (a,b) DJF for the North Atlantic and (c,d) JJA for the South Atlantic, for the (a,c) cyclogenesis and (b,d) storm track. The density difference unit is cyclones/track per month per area, where the unit area is equivalent to a 5° spherical cap (10^6 km^2). The dots represent grid points where the trend is significant within 99% confidence level, and the differences are CFSR/CFSv2 minus ERA5 considering 1979-2019 period.

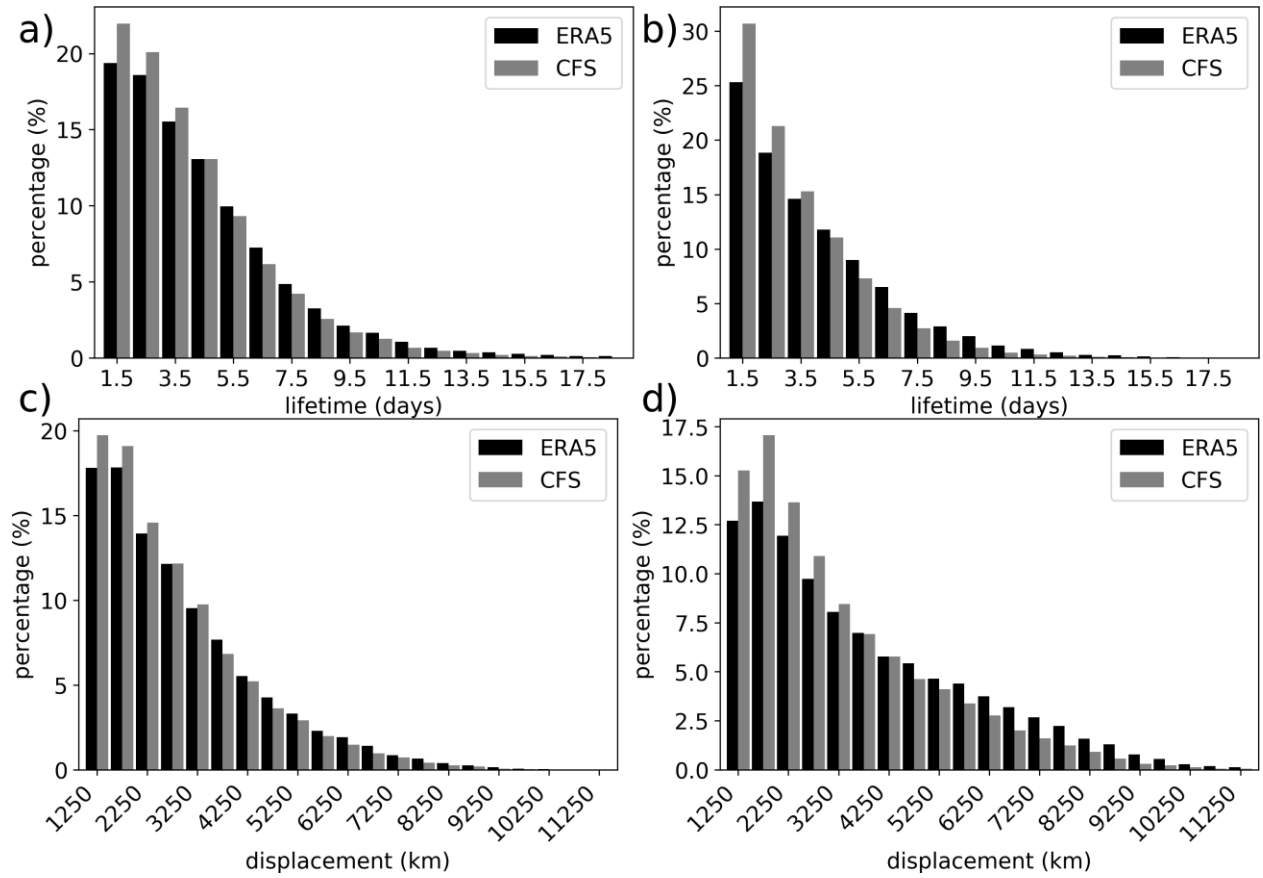


Figure 7 Histograms of cyclones (a,b) lifetime (days), and (c,d) displacement (km).for the (a,c) North Atlantic and (b,d) South Atlantic Oceans. The histograms were computed considering the whole 1979-2019 period for the ERA5 (black) and CFSR/CFSv2 (grey).

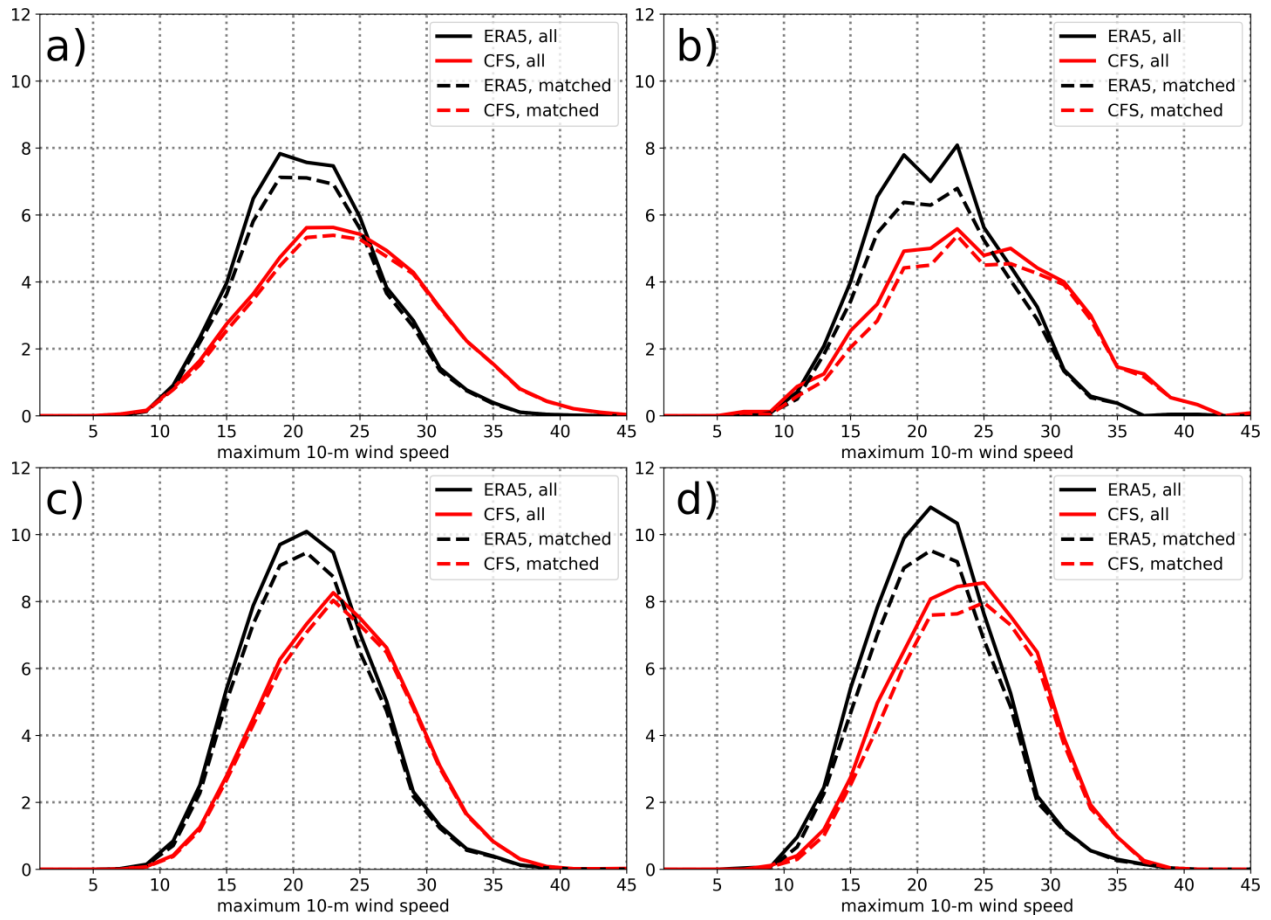


Figure 8. Cyclone's maximum 10-meters wind speed (m s⁻¹) distribution for the (a,b) North Atlantic in DJF, and (c,d) South Atlantic in JJA, considering the period between (a,c) 1979 and 2019, and (b,d) April/2011 and 2019. ERA5 distributions are in black, and CFSR/CFSv2 are in red. The dashed lines are the distributions computed for the matched cyclones in each dataset. The y-axis is cyclone per month.